

## Cerium-doped Mn<sub>2</sub>O<sub>3</sub> Microspheres: A High-performance Cathode Material for Aqueous Zinc-ion Batteries

*Xin Li<sup>a</sup>, Wenyu Wang<sup>a</sup>, Linwen Li<sup>b</sup>, Chengyu Xue<sup>a</sup>, Yang Chen<sup>a</sup>, Tiantian Zhu<sup>a</sup>,*

*Fuxiang Wei<sup>a,\*</sup>, Yanwei Sui<sup>a</sup>, Jie He<sup>b</sup>, Zunyang Zhang<sup>b</sup>*

*<sup>a</sup>School of Materials and Physics, China University of Mining & Technology,*

*Xuzhou · 221116, PR China*

*<sup>b</sup>Xuzhou Huaihai New Energy Vehicle Parts Co., Ltd, Xuzhou, 221116, PR China*

*\* Corresponding author*

*Fuxiang Wei: weifuxiang2001@163.com*

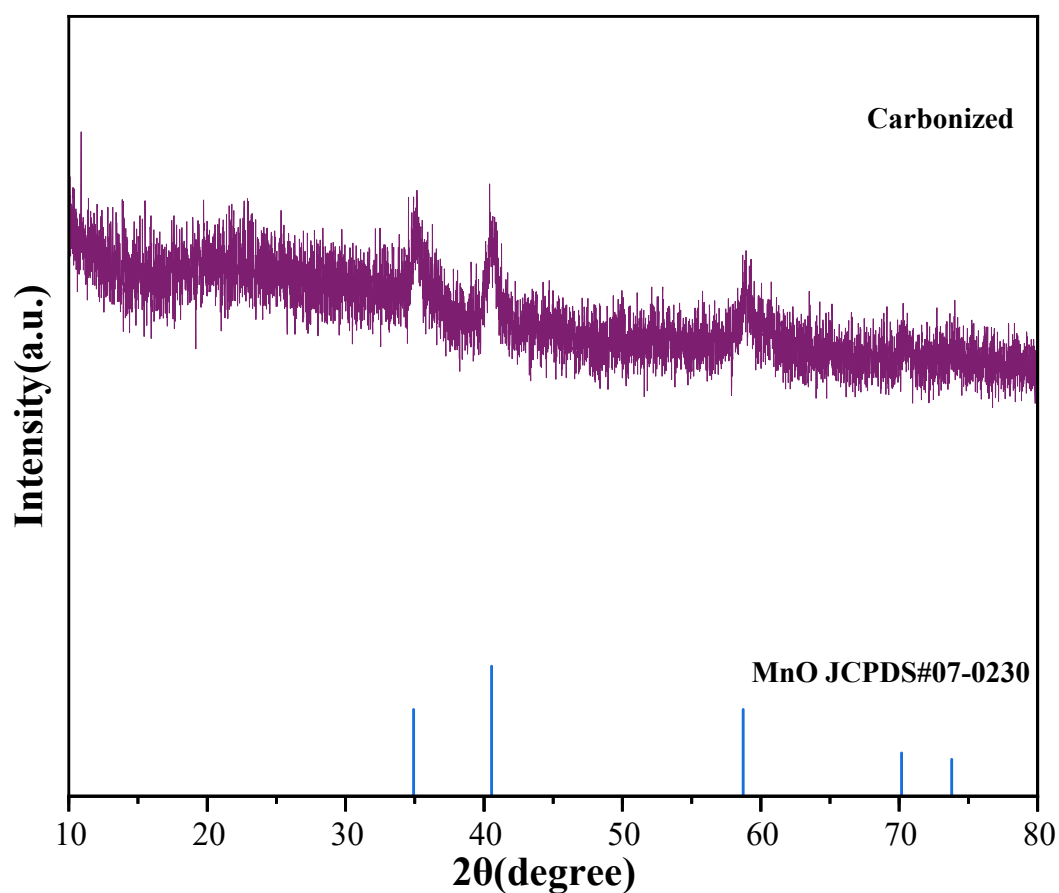


Fig. S1 XRD spectra of carbonized MnBTC

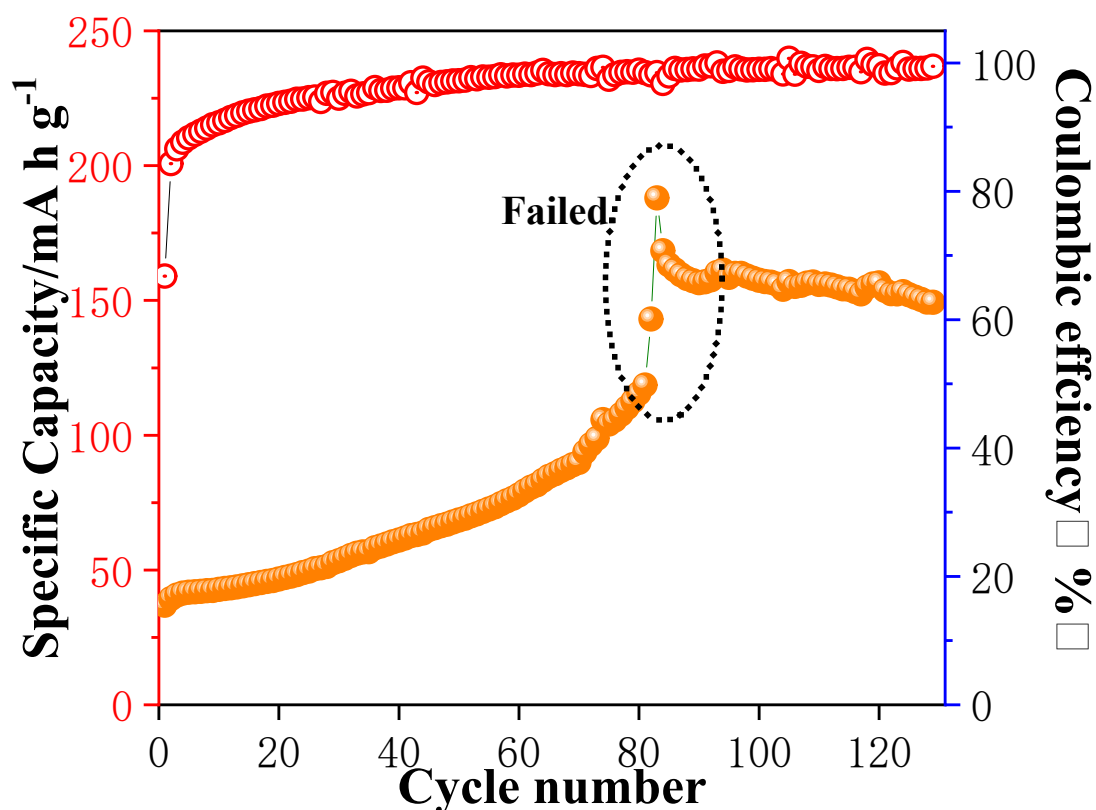


Fig. S2 cycling performance data of MnBTC after carbonization

#### Ex-situ XRD patterns of Ce-Mn<sub>2</sub>O<sub>3</sub> cathodes

In the study of the Zn<sup>2+</sup> storage mechanism of Ce-Mn<sub>2</sub>O<sub>3</sub> cathode materials, the phase composition of the material at different charge-discharge states was examined through ex-situ XRD testing. **Fig. 8 (a)** displays the galvanostatic charge-discharge (GCD) curves at a current density of 0.1 A g<sup>-1</sup>, with different voltage points indicated. **Figure 8 (b)** illustrates the XRD patterns of the Ce-Mn<sub>2</sub>O<sub>3</sub> cathode at various voltage points. The initial state I<sub>s</sub> exhibits diffraction peaks for titanium foil and Mn<sub>2</sub>O<sub>3</sub>. Upon discharging to 1.1 V (I), 1.0 V (II), and 0.8 V (III), the formation of a new phase, Zn<sub>4</sub>SO<sub>4</sub>(OH)<sub>6</sub>·4H<sub>2</sub>O, is observed, with its diffraction peaks intensifying as the voltage decreases, reaching a maximum at 0.8 V. Upon charging to 1.4 V (IV), 1.6 V (V), and 1.9 V (VI), the diffraction peaks of Zn<sub>4</sub>SO<sub>4</sub>(OH)<sub>6</sub>·4H<sub>2</sub>O gradually diminish, almost vanishing at 1.9 V, indicating the reversibility of the material. Upon re-discharging to 0.8 V (VII), the phase reappears, further confirming the reversibility of the material. These results suggest that the Ce-Mn<sub>2</sub>O<sub>3</sub> cathode involves a co-intercalation/de-intercalation mechanism of Zn<sup>2+</sup> and H<sup>+</sup> during the charge-discharge process.

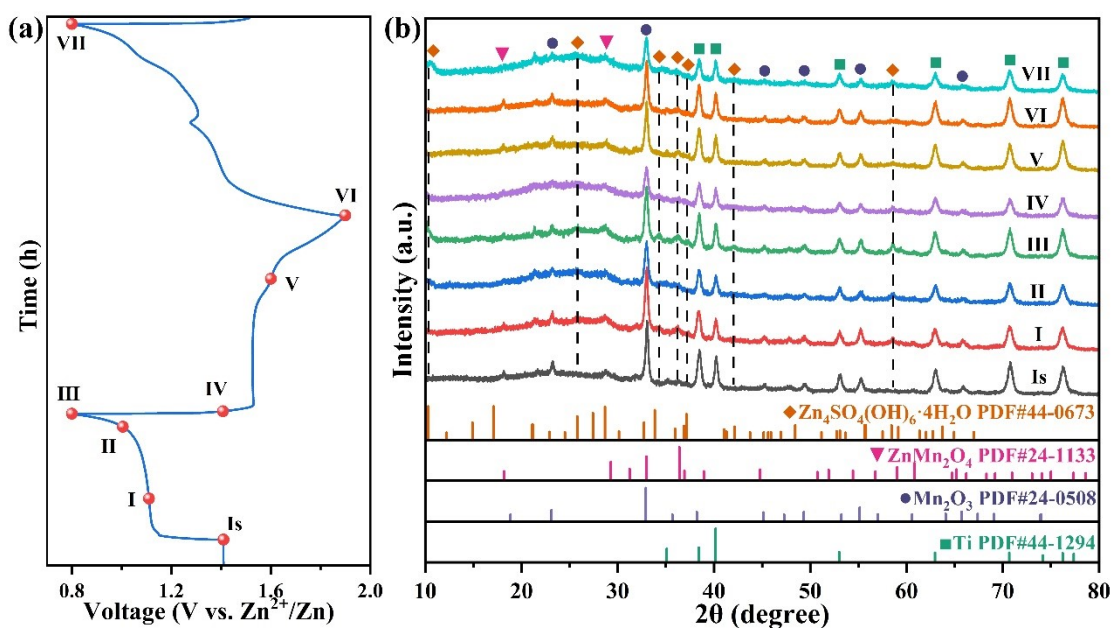


Fig. S3 (a) Constant-current charge/discharge curve of Ce-Mn<sub>2</sub>O<sub>3</sub> anode at 0.1 A g<sup>-1</sup> current density; (b) Ex-situ XRD patterns of Ce-Mn<sub>2</sub>O<sub>3</sub> cathodes

Materials	Current density (mA g <sup>-1</sup> )	Cycle numbers	Reversible capacity (mAh g <sup>-1</sup> )	Reference
δ-MnO <sub>2</sub>	83	100	112	1
D-β-MnO <sub>2</sub>	500	300	200	2
Mn <sub>3</sub> O <sub>4</sub> @NC	1000	700	97	3
O <sub>Cu</sub> Mn <sub>2</sub> O <sub>3</sub>	1000	600	95	4
Ce-Mn <sub>2</sub> O <sub>3</sub>	1,000	1000	114.4	This work

Table S1 Comparison on discharge reversible capacity and cycling performance between our work and resent Mn-based publications

#### Supplementary reference

- 1 M. H. Alfaruqi, J. Gim, S. Kim, J. Song, T. P. Duong, J. Jo, Z. Xiu, V. Mathew and J. Kim, *Electrochem. Commun.*, 2015, **60**, 121–125.
- 2 M. Han, J. Huang, S. Liang, L. Shan, X. Xie, Z. Yi, Y. Wang, S. Guo and J. Zhou, *iScience*, 2020, **23**, 100797.
- 3 M. Sun, D.-S. Li, Y.-F. Wang, W.-L. Liu, M.-M. Ren, F.-G. Kong, S.-J. Wang, Y.-Z. Guo and Y.-M. Liu, *ChemElectroChem*, 2019, **6**, 2510–2516.
- 4 N. Liu, X. Wu, Y. Yin, A. Chen, C. Zhao, Z. Guo, L. Fan and N. Zhang, *ACS Appl. Mater. Interfaces*, 2020, **12**, 28199–28205.